Clofazimine treatment modulates key non-coding RNAs associated with tumor progression and drug resistance in lethal Prostate Cancer

Sarah Batten[1]#, Harish Kumar[1,2]#, Suman Mazumder[1,3], Taraswi Mitra Ghosh[4], Amit Kumar Mitra[1,3*]

[1]Department of Drug Discovery & Development, Harrison College of Pharmacy, Auburn University, AL; [2]Division of Hematology and Oncology, University of Alabama at Birmingham, Birmingham, AL; [3]Center for Pharmacogenomics and Single-Cell Omics Initiative, Auburn University, Auburn, AL; [4]Department of Urology, Mass General Brigham and Women's Hospital and Department of Surgery, Harvard Medical School, Boston, MA

#Contributed equally

***Corresponding Author:**

Amit Kumar Mitra, PhD

Associate Professor, Drug Discovery and Development

Director, Center for Pharmacogenomics and Single-Cell Omics (AUPharmGx)

Harrison School of Pharmacy

Auburn University

3306D Walker Building

Auburn, Alabama 36849

Office: 334.844.7404

Email: akm0060@auburn.edu

Running title: Preclinical development of Clofazimine in lethal PCa

Keywords: mCRPC, Clofazimine, RNAseq, lncRNA, Taxane resistance, Combination therapy

Word count: 3463

Tables: 2

Figures: 7

References: 28

ABSTRACT

Prostate cancer (PCa) is the most commonly diagnosed cancer and the second-leading cause of cancer death among men in the United States, representing 24.3% of all new cancer cases in the US Metastatic castration-resistant prostate cancer (mCRPC) is a lethal variant of prostate cancer that is associated with increased aggressiveness, cancer stemness, morbidity, and the risk of developing into taxane drug-resistant PCa. As taxanes are currently the first-line chemotherapeutic agents for mCRPC, there is a critical need to develop novel agents for the treatment of mCRPC. Clofazimine (CLF) is a potential immunomodulator drug that is FDA-approved for the treatment of leprosy.

Recently, using a phenotype-based high-throughput drug screening, we demonstrated the *in vitro* (cell lines), *in vivo* (mouse xenograft models), and *ex vivo* (patient-derived primary tumor cells) efficacy of CLF in drug-resistant forms of chronic myeloid leukemia and multiple myeloma.

In this study, we demonstrate that CLF is effective as a single agent and in combination with docetaxel (DTX) in a panel of PCa cell lines representing the diversity of CRPC patients. The response to CLF in the PCa cell lines was quantified using *in vitro* cytotoxicity assays, caspase 3/7 activity assay for apoptosis, cell cycle analysis, and aldehyde dehydrogenase activity assay for cancer stemness. We show that following CLF treatment, cellular pathways associated with apoptosis and ER stress were up-regulated, providing additional understanding of the mechanism of action of CLF in PCa cells. Further, we also found that CLF reduces ALDH activity, which is a marker for cancer cell stemness, a subtype of cancer cells that are associated with the aggressiveness of the cancer.

Finally, drug-induced changes were investigated using whole transcriptome (next-generation RNA sequencing) analysis, where CLF treatment was found to modulate the expression of several non-coding RNAs that are associated with tumor cell proliferation, cell migration, and PCa drug resistance. Western Blotting was performed to validate the dysregulation of proteins associated with cell death and apoptosis, as well as the top dysregulated pathways in mCRPC following treatment with CLF.

Our results support the preclinical development of CLF as a combination therapy candidate against aggressive forms of Prostate Cancer and provide additional insights into its mechanism of action.

INTRODUCTION

Prostate cancer (PCa) is among the most common cancers in the United States and globally, with the American Cancer Society estimating that in 2024, there will be 299,000 new PCa cases and 35,000 deaths from PCa in the US alone (*Prostate Cancer Facts, American Cancer Society*, 2024). Globally, the World Cancer Research Fund International reported 1.47 million new PCa cases and 397,000 deaths from PCa in 2022 (Prostate Cancer Statistics, *World Cancer Research Fund*, 2024). While the majority of PCa tumors are adenocarcinomas, the most lethal sub-types of PCa are the metastatic castration-resistant PCa (mCRPC) subtypes[1]. 10-20% of PCa cases develop castration resistance within 5 years of the initial diagnosis, with this progression typically occurring after 2-3 years of hormonal manipulation[2], [3]. Taxanes are the first-line chemotherapeutics for mCRPC, but many patients develop taxane resistance, limiting the efficacy of this treatment [4]. Given the increase in PCa incidence and the growing problem of taxane resistance, targeted novel or repurposed drugs are needed to combat these trends. From a cost and time standpoint, repurposing drugs that already have FDA approval for other disease states presents an important next step in chemotherapeutic development.

Clofazimine (CLF) is a derivative of riminophenazines, initially isolated from lichens. It was developed and is FDA-approved for the treatment of leprosy and is being repositioned for the treatment of multidrug-resistant tuberculosis [5]. We had previously identified CLF through high-throughput screening as a potentially efficacious agent for treating chronic myeloid leukemia (CML)[6]. While the exact mechanisms of action of CLF are under investigation, CLF has been shown to activate the peroxisome proliferator-activated receptor-gamma (PPAR-γ) and synergize with tyrosine-kinase inhibitors in the treatment of CML[7]. Additionally, we showed CLF exhibits a synergistic effect in combination with standard-of-care drugs in the treatment of multiple myeloma, specifically in the treatment of PI and IMiD-resistant myeloma[8]. Integrating *in vitro* and *ex vivo* model systems with bulk and single-cell -omics, we identified novel pathways associated with CLF efficacy, including induction of ER stress, autophagy, mitochondrial dysfunction, oxidative phosphorylation, enhancement of downstream cascade of p65-NFkB-IRF4-Myc downregulation, and ROS-dependent apoptotic cell death in myeloma[8]. Recently, a phenotype-based screen identified several therapeutic agents selective for metastatic Prostate Cancer, including CLF[6]. However, no other study so far has explored the functional consequences of Clofazimine treatment specific to prostate cancer.

Due to the effectiveness of CLF against the aggressive, drug-resistant, and 'stem-like' forms of various cancers, this study focuses on the effects of CLF against a panel of PCa cell lines representing the diversity of patients with lethal PCa. Furthermore, we show that Clofazimine treatment downregulates several non-coding RNAs that have been shown to be associated with tumor cell proliferation, cell migration, invasion, and drug resistance in prostate cancer.

MATERIALS AND METHODS

Human Prostate Cancer Cell Lines

AR^{lo} mCRPC/NEPC cell lines (PC3, PC3M, DU145) and the osteotropic subline, C42b, were obtained from the American Type Culture Collection (ATCC; Manassas, VA, USA). The taxane-resistant cell line DUTXR was generated using dose-escalation of taxanes over time. The cell lines were authenticated at the source and tested randomly at regular intervals for tissue specimen provenance and cell lineage at the AU Center for Pharmacogenomics and Single-Cell Omics (AUPharmGx) using the GenePrint 24 System (Promega; Madison, WI, USA). All cell lines are mycoplasma negative. The cell lines were maintained in an incubator at 37°C with 5% CO_2 using the recommended ATCC media for each cell line supplemented with 10% FBS and Penicillin-Streptomycin.

Drugs and Reagents

The drugs, reagents, and kits that were used are listed in **Table 1**. All drugs were solubilized in dimethyl sulfoxide (DMSO, Sigma-Aldrich; St. Louis, MO, US) and stored at -20°C.

In Vitro Cytotoxicity Assays

PCa cell lines were treated with serial dilutions containing decreasing concentrations of CLF and DTX, as single-agent and combination therapy, for 48 hours. Cytotoxicity assays were performed using Resazurin cell viability assay (Ward's Science; Rochester, NY, USA). Absorbance was measured using a Neo2 Microplate Reader (Biotek; Winooski, VT, USA). The half-maximal inhibitory concentration (IC_{50}) values were calculated by nonlinear regression using a sigmoidal dose-response equation. These values were used to compare the dose-response of single-agent and combination therapies. Drug synergy was calculated by comparing single-agent and combination drug-response data based on Chou-Talalay's combination index (CI) method and the isobologram algorithm (CompuSyn software; Biosoft, US[9,10]. CI values between 0.9-0.3 and 0.3-0.1 signify synergism and strong synergism, respectively, between the drugs treated in combination.

Apoptosis Assays

PCa cells were cultured for 48h in the presence of indicated concentrations of CLF and DTX as single agents and, in combination, harvested, washed, and incubated with Annexin V-FITC and Propidium Iodide for 15min at room temperature in the dark following the manufacturer's protocol (BD Biosciences; Franklin Lakes, NJ, USA). Apoptosis was measured by BD LSR II flow cytometry (BD Biosciences; Franklin Lakes, NJ, USA) and analyzed using FlowJo™ Software (Ashland, OR, USA).

Caspase-3/7 activity assay was performed on the PCa cell lines using Caspase-Glo 3/7 luminescent assay kit according to the manufacturer's instructions (Promega; Madison, WI, USA). Briefly, $1x10^6$/mL cells were cultured in 6 well plates and treated with either CLF alone or in combination with DTX for indicated times. After harvesting, cells were washed twice with cold PBS and resuspended with Caspase-glo 3/7 agents. Reactions were incubated for 1h at 37°C, and luminescence was determined using a Synergy 2 Microplate Reader (Biotek; Winooski, VT, USA). Cell death by apoptosis was also measured using immunoblotting analysis.

Aldeflour Activity Assay

Aldehyde dehydrogenase (ALDH) activity was assessed using the ALDEFLUOR ™ assay kit according to the manufacturer's instructions (Stem Cell Technologies; Vancouver, Canada). Briefly, $1x10^6$ PCa cells were treated with CLF-based regimens for 24h, harvested, and resuspended in 1 mL Aldefluor assay buffer containing the ALDH substrate BODIPY-aminoacetaldehyde (BAAA). Negative control samples were treated with 5 µL of diethylaminobenzaldehyde (DEAB) as an inhibitor of ALDH1 enzymatic activity. Cells were incubated for 30-45 minutes at 37 °C, washed twice, and suspended in Aldefluor assay buffer. The brightly fluorescent ALDH+ cells were detected by BD LSR II flow cytometer (BD Biosciences; Franklin Lakes, NJ, USA) and analyzed using FlowJo™ Software (Ashland, OR, USA).

DCFDA Total Cellular Reactive Oxygen Species (ROS) assay

PCa cells were treated for 24hrs with DTX, CLF, and DTX+CLF combination. Following 24hrs, cells were incubated with 10µM DCFDA in RPMI (Phenol red-free) medium at 37°C for 30min, washed twice with phosphate buffer saline (PBS). ROS production was measured using Synergy Neo2 Microplate Reader (Biotek).

Detection of the Mitochondrial Membrane Potential (MMP)

Untreated, DTX-treated, CLF-treated, and DTX+CLF combination-treated (24hrs) cells were incubated with 5µM JC-1 dye for 15 min in the dark at 37°C and washed twice in PBS. Mitochondrial Membrane Potential was then assayed using Synergy Neo2 Microplate Reader (Biotek).

Gene Expression Profiling (GEP) Analysis

Cells were plated at a density of $4x10^5$/mL cells and were treated with CLF. After 24h incubation, high-quality RNA was isolated using QIAshredder and RNAeasy kit (Qiagen; Hilden, Germany). RNA concentration and integrity were determined using the Nanodrop-8000 (Thermo-Fisher Scientific; Waltham, MA, US) and Agilent 2100 Bioanalyzer (Agilent Technologies; Santa Clara, CA, US) and stored at -80 °C. An RNA integrity number (RIN) threshold of 8 was used for RNA-seq analysis. RNA-seq libraries were constructed using Illumina TruSeq RNA sample preparation kit v2 (Illumina; San Diego, CA). Next-generation RNA sequencing was performed on Illumina's NovaSeq platform using a 150bp paired-end protocol with a depth of > 20 million reads per sample.

RNAseq Data Analysis

Gene expression profiling (GEP) data was pre-processed and filtered (genes with mean counts<10 were removed), and the normalized (CPM - counts per million) data was analyzed using the Partek Flow package (Partek, Inc; St. Louis, MO, USA) to perform differential expression testing to identify GEP signatures. Least squares (LS) mean values were calculated for each group as the linear combination or sum of the estimated means from the linear model. LS mean is model-dependent and produces a more accurate, unbiased estimate of the group means even in unbalanced data. An LS Mean threshold of >=1 was applied for analysis, and differential gene expression analysis between groups was performed using limma, an empirical Bayesian method, to detect differentially expressed (DE) genes. The advantage of limma compared to traditional t-tests is the limma provides moderated t-test statistic by shrinking the variances statistics, therefore improving the statistical power[8]. Mean fold-change>|1| and $p<0.05$ were considered as the threshold for

reporting significant differential gene expression. Heatmaps were generated using unsupervised hierarchical clustering (HC) analysis based on the top DE genes.

Pathway analysis

IPA software (Qiagen; Hilden, Germany) was used to identify i) the most significantly affected molecular pathways, ii) upstream regulator molecules like microRNA and transcription factors, iii) downstream effects and biological processes, and iv) causal networks predicted to be activated or inhibited in response to treatment based on the most significant DE genes. Furthermore, additional pathway analyses were performed using the web-based tool gProfiler and Gene Set Enrichment Analysis (GSEA) based on the MSigDB database enrichment background.

Patient Dataset

Gene expression on Prostate Adenocarcinoma patients included in The Cancer Genome Atlas (TCGA) database (TCGA-PRAD) was extracted from the Genomic Data Commons (GDCs) server (cancergenome.nih.gov). The interactive web-based tool Gene Expression Profiling Interactive Analysis (GEPIA) was used for in-depth analysis of TCGA gene expression data files and to compare transcriptome data on target candidate pathway genes with patient survival (overall survival (OS) or disease-free survival (DFS)) from the prostate expression data matrix[11].

Statistical Analysis

All statistical analysis was performed using R v4.3.2 and GraphPad Prism v10. All tests were two-sided, with $p<0.05$ being considered statistically significant.

RESULTS

CLF treatment results in loss of viability and increased apoptosis in PCa cell lines, as single-agent and in combination with Taxanes

The effectiveness of CLF was first evaluated using *in vitro* cytotoxicity assays in our PCa cell line panel, which represents the representing the broad spectrum of biological and genetic heterogeneity of PCa patients, including non-metastatic and metastatic disease, as well as innate and acquired taxane resistance. We observed that single-agent CLF treatment showed a reduction in cell viability following 48h of treatment, which was further enhanced when CLF was combined with DTX, which is a primary drug for CRPC (**Figure 1A**). Drug synergy analysis using Chou-Talalay's combination index (CI) method (CompuSyn software; Biosoft, US showed a CI value of 0.028 for PC3 and 0.278 for DU145, indicating strong synergism[9,10]. Furthermore, the Dose reduction index (DRI) for DTX was 37.991 for PC3 and 4.504 for DU145, suggesting that combination therapy with CLF reduces the dose requirement of DTX.

Next, we tested the impact of CLF treatment on cellular apoptosis in the PCa cell line panel. Using Annexin V-PI staining, we showed that treatment with CLF as a single agent resulted in elevated levels of apoptosis in PCa lines compared to no-drug control. Further, the percentage of apoptotic cells in each cell line tested was considerably increased following CLF+DTX combination treatment compared to single-agent treatment (**Figure 1B)**. Our results were confirmed using Caspase 3/7 activity assay (**Figure 1C**).

CLF inhibited aldehyde dehydrogenase activity in PCa cells

ALDH has been shown to be associated with 'cancer stemness' and resistance to taxane therapy in prostate cancer. **Figure 2** shows higher baseline aldehyde dehydrogenase (ALDH) activity level in the clonally derived taxane-resistant mCRPC cell line DUTXR compared to the parental line (DU145). This is a significant finding as ALDH is an intracellular enzyme that is frequently over-expressed in cancer stem cells and has been linked to drug resistance. Further, we showed (**Figure 2A-E**) that treatment with CLF reduced ALDH activity in the PCa cell lines tested when compared to the no-treatment control.

Gene expression profiling revealed genes and molecular pathways/networks associated with CLF treatment in lethal PCa

Next, we performed genome-wide transcriptome (next-generation mRNA sequencing or RNAseq) analysis to identify genes that were differentially regulated following CLF treatment. Volcano plots showing these differentially expressed (DE) genes are provided in **Figure 3A.** Among these, 557 genes were shown to be significantly differentially regulated following CLF treatment with ($p<0.05$; fold-difference ≠ 1; 260 Up-regulated and 297 down-regulated). Of these genes, 497 had an absolute fold-change ≥ 2 (243 Up-regulated and 254 down-regulated). The Venn diagram in **Figure 3B** shows that among the genes that were differentially regulated following CLF treatment (fold change ≠ 1), 1027 were common between all the mCRPC cell lines

(PC3, PC3M, and DU145). **Figure 3C** shows a heatmap representing the top genes that were significantly differentially expressed between CLF-treated vs untreated controls.

Pathway analysis revealed top differentially regulated canonical pathways associated with PCa cells treated with CLF

A graphical summary of the IPA analysis based on differentially regulated genes following CLF treatment in PCa cell lines is shown in **Figure 4A**, where orange indicates predicted activation and blue predicted inhibition. Top differentially regulated canonical pathways associated with CLF treatment include oxidative phosphorylation, autophagy, and mitochondrial dysfunction, as shown in **Figure 4B**. **Figure 4C** represents the top upstream regulators predicted to be activated or inhibited following single-agent CLF treatment.

Confirmation of CLF-induced effects on altered mitochondrial metabolism

We assessed the CLF treatment-induced change in mitochondrial membrane potential using JC-1 (Sigma). JC-1 is a cationic fluorescent dye that accumulates at a higher level in the mitochondria of cancer cells, representing elevated mitochondrial membrane potential ($\Delta\Psi$), which may be the result of enhanced oxidative phosphorylation. This accumulation of JC-1 leads to the formation of J-aggregates, which can be assayed through red fluorescence (emission maximum at 590 nm) compared to the green fluorescence of J-monomers. Further, we used DCFDA (Sigma) to measure intracellular ROS levels and confirm the effect of CLF on reactive oxygen species (ROS), like superoxides and hydrogen peroxide (H_2O_2). Representative plots demonstrate that CLF treatment results in mitochondrial membrane depolarization (**Figure 5A**) and affects intracellular ROS production (**Figure 5B**). Similar results were also obtained for the other PCa cell lines (data not shown).

Validation of CLF Treatment-Induced differential gene signature using TCGA-PRAD dataset

In silico analysis using TCGA's prostate adenocarcinoma (PRAD) GEP dataset showed that several genes that were significantly differentially dysregulated following CLF treatment were also significantly associated with disease-free survival (Kaplan-Meier curves – **Figure 6**), with Hazards Ratios >2 and $p<0.05$. Thus, these biomarkers may serve as additional cues to the mechanism of action of Clofazimine, which is specific to its efficacy in metastatic/aggressive PCa.

DISCUSSION

There is a spectrum of responses to taxane therapies among mCRPC patient populations due to variations in biological and genetic factors, but DTX resistance inevitably occurs [12]. Drug resistance severely limits the efficacy of current chemotherapeutics, with the exact mechanisms and development of resistance still not yet being fully understood [4]. In this study, we have shown that CLF induces significant cytotoxicity in PCa cell lines, including DTX-resistant lines, as single-agent and synergistically, in combination with standard-of-care treatments, which could be used as a therapeutic strategy for overcoming taxane resistance. Next, using cell-based studies and RNAseq-based next-generation gene expression profiling, we have provided additional insights into the mechanism of action for CLF in PCa.

Earlier studies have shown that CLF functions as a broad-spectrum antibiotic by generating reactive oxygen species, superoxide, and hydrogen peroxide, as well as exhibiting anti-inflammatory properties for leprosy and auto-immune diseases [5]. CLF's potential for the treatment of mCRPC was initially identified through an unbiased phenotype-based screen that analyzed 1,120 different compounds, where CLF showed preferential cytotoxicity and apoptotic effects for mCRPC cells, both *in vitro* and *in vivo* [6]. As no previous studies have further explored the effects of CLF in PCa cells, our work has extended knowledge on this potential therapeutic strategy, as well as investigating the possible synergistic effects of CLF and DTX in PCa cell lines. Through using integrated -omics-based strategies, the mechanism of action of CLF has been explored.

CLF's potential for the treatment of mCRPC was validated through *in vitro* chemosensitivity assays, where it was shown that CLF induces cytotoxicity and caspase-dependent apoptosis in PCa cell lines, both as a single agent and in combination with DTX. While the CLF doses that showed synergy were in the micromolar concentration range, they are within the safe and well-tolerated dose range of 0.84-8.4 µM, corresponding to a human C_{max} of 0.4-4 mg/L [5]. The potential synergistic effects of CLF with DTX for mCRPC cases is an avenue for further exploration through patient-derived xenograft *in vivo* models.

We also showed that CLF reduces aldehyde dehydrogenase (ALDH) activity significantly in our panel of PCa cell lines as compared to control cells. ALDH is a surface marker that characterizes cancer stem cells (CSCs), which are defined as malignant tumor cells with a high potential for self-renewal and differentiation[13]. CSCs derived from PCa express ALDH, and chemotherapeutic resistance can be induced by CSCs through ROS generation and ALDH activity[13]. Treatment of our panel of PCa cell lines with CLF reduced ALDH activity significantly in most cell lines, including notably by 67.86% in the taxane-resistant cell line.

We have previously shown in chronic myeloid leukemia and multiple myeloma studies that CLF modulates PPARγ ubiquitin ligase activity, which results in ROS-mediated apoptosis [7], [14]. PPARγ functions as a

tumor suppressor in PCa that induces inhibition of cell growth, decreased tumor invasiveness, and decreased production of proinflammatory cytokines [15]. Here, using gene expression profiling analysis, we validated the PPARγ pathway as the mechanism of action for CLF, as several of the top differentially regulated genes are related to cellular stress pathways that are modulated by PPARγ. For example, CHAC1, which is induced following unfolded protein response, showed a positive fold change of 16.42 following CLF treatment. CHAC1 modulates several pro-apoptotic transcription factors, including ATF3 and CHOP, and thus, the up-regulation of CHAC1 is connected to increased apoptotic activity [16]. DDIT4 displayed a positive fold change of 12.20 when PCa cells were treated with CLF. This protein-coding gene is associated with the mTOR signaling pathway. Overexpression of DDIT4 is induced under cellular stress and contributes to stress-induced responses, including autophagy and apoptosis [17].

Most importantly, CLF treatment was found to modulate the expression of several non-coding RNAs that are associated with tumor cell proliferation, cell migration, invasion, and PCa drug resistance. The top differentially regulated non-coding RNAs that are most relevant to this study are represented in **Figure 7** (**Table 2**). These include long non-coding RNAs, snRNAs, and RNA adjuvants. The overexpression of MALAT1 is associated with increased cell proliferation, invasion, metastasis, evasion of apoptosis, and drug resistance through the regulation of several cell-signaling pathways[18]. We found that MALAT1 expression was significantly downregulated (fold-change 18.06) when PCa cells were treated with CLF. Higher levels of NEAT1 are known to indicate poor survival in cancer patients, associated with bone metastasis in PCa patients, and reduce sensitivity to chemotherapy[19].

Treatment with CLF was found to decrease the level of NEAT1 > 8.01 folds. RTCA-AS1, which is associated with pathological grade oral and oropharyngeal squamous cell carcinoma, is decreased by a fold change of 4.28 in CLF-treated PCa cells[20]. LINC00973 is a lncRNA that is over-expressed following DNA damage and has anti-proliferative and pro-apoptotic functions through inhibition of p21 degradation[21]. After CLF treatment of PCa cells, the level of LINC00973 present was increased by a fold-change of 6.55. Additionally, RN7SK is a lncRNA that has been shown to be associated with a positive feedback circuit through interaction with m6A readers in tumor cells, which increases cellular proliferation[22]. PCa cells treated with CLF downregulated the expression of RN7SK by greater than 10-fold (Fold change -10.29) compared to untreated control. STAG3L5P-PVRIG2P-PILRB is up-regulated in bladder cancer and has been identified as a prognostic necroptosis-related lncRNA[23]. Treatment with CLF for PCa cells decreased the expression of STAG3L5P-PVRIG2P-PILRB (Fold-change -3.85). LOXL-AS1 is known to regulate gene expression and signaling pathways through binding to microRNAs, affecting cell proliferation, migration, invasion, and apoptosis[24]. It is also up-regulated in multiple cancers, including PCa, and is positively associated with adverse clinical signs in cancer patients[24]. LOXL-AS1 expression was decreased in CLF-treated PCa cells by ~3 folds (Fold change -2.90). LINC00342 has shown a correlation between its overexpression and poor prognosis of patients with clear cell renal cell carcinoma, likely due to its role in the reprogramming of glucose metabolism and cancer metastasis[25]. MIR210HG is a lncRNA whose high expression in several cancers is associated with cell proliferation, invasion, migration, and energy metabolism[26]. In PCa, it has been correlated with facilitating PCa progression[27]. After treating PCa cells with CLF, the expression of MIR210HG was decreased by ~3 folds (Fold change -3.05). Finally, OLMALINC is

thought to be related to the immune microenvironment of some cancers, with it being found to positively relate to mast cell activation in osteosarcoma patients[28]. In PCa cells treated with CLF, expression of OLMALINC was found to increase by a fold-change of 3.84.

As CLF is an FDA-approved low-cost medication that is well-tolerated in patients, repurposing CLF as a secondary agent in the treatment of mCRPC is an exciting potential approach for targeting drug-resistant mCRPC.

Authorship Contributions

S.B, H.K, T.M.G., and A.K.M. participated in the research design; S.B, H.K, S.M., T.M.G. conducted experiments: S.B, H.K, T.M.G., and A.K.M. performed data analysis; S.B, T.M.G., and A.K.M. wrote or contributed to the writing of the manuscript; A.K.M. supervised the overall project. All authors have read and agreed to the published version of the manuscript.

Data Availability Statement

The datasets generated during and/or analyzed during the current study are available from the corresponding author upon reasonable request.

Conflicts of Interest

All authors have read the journal's policy on the disclosure of potential conflicts of interest. The authors declare that they have no competing interests.

Funding Statement

This research received no external funding.

REFERENCES

1 Wasim, S., Lee, S.-Y. & Kim, J. Complexities of Prostate Cancer. *International Journal of Molecular Sciences* **23**, 14257 (2022). https://doi.org/10.3390/ijms232214257

2 Velky, J. E. & Ricke, W. A. Development and prevalence of castration-resistant prostate cancer subtypes. *Neoplasia* **22**, 566-575 (2020). https://doi.org/10.1016/j.neo.2020.09.002

3 Yehya, A. *et al.* Drug resistance in metastatic castration-resistant prostate cancer: an update on the status quo. *Cancer Drug Resistance* **5**, 667-690 (2022). https://doi.org/10.20517/cdr.2022.15

4 Cai, M. *et al.* Current therapy and drug resistance in metastatic castration-resistant prostate cancer. *Drug Resistance Updates* **68** (2023). https://doi.org/10.1016/j.drup.2023.100962

5 Xu, J., Koval, A. & Katanaev, V. L. Clofazimine: A journey of a drug. *Biomedicine & pharmacotherapy* **167** (2023).

6 Chung, I. *et al.* Unbiased Phenotype-Based Screen Identifies Therapeutic Agents Selective for Metastatic Prostate Cancer. *Frontiers in Oncology* **10** (2021).

7 Kumar, H. *et al.* Leprosy drug clofazimine activates peroxisome proliferator-activated receptor-gamma and synergizes with imatinib to inhibit chronic myeloid leukemia cells. *Haematologica* **105** (2020).

8 Kumar, H. *et al.* Single-Cell Proteomics and Tumor RNAseq Identify Novel Pathways Associated With Clofazimine Sensitivity in PI- and IMiD- Resistant Myeloma, and Putative Stem-Like Cells. *Front Oncol* **12**, 842200 (2022). https://doi.org/10.3389/fonc.2022.842200

9 Chou, T. C. & Talalay, P. Quantitative analysis of dose-effect relationships: the combined effects of multiple drugs or enzyme inhibitors. *Adv Enzyme Regul* **22**, 27-55 (1984). https://doi.org/10.1016/0065-2571(84)90007-4

10 Chou, T. C. Drug combination studies and their synergy quantification using the Chou-Talalay method. *Cancer Res* **70**, 440-446 (2010). https://doi.org/10.1158/0008-5472.CAN-09-1947

11 Tang, Z. *et al.* GEPIA: a web server for cancer and normal gene expression profiling and interactive analyses. *Nucleic Acids Res* **45**, W98-W102 (2017). https://doi.org/10.1093/nar/gkx247

12 Maloney, S. M., Hoover, C. A., Morejon-Lasso, L. V. & Prosperi, J. R. Mechanisms of Taxane Resistance. *cancers* **12** (2020). https://doi.org/10.3390/cancers12113323

13 Zeng, Z. *et al.* Regulation and signaling pathways in cancer stem cells: implications for targeted therapy for cancer. *Molecular Cancer* **22** (2023). https://doi.org/101186/s12943-023-01877-w

14 Kumar, H. *et al.* Single-Cell Proteomics and Tumor RNAseq Identify Novel Pathways Associated With Clofazimine Sensitivity in PI- and IMiD- Resistant Myeloma, and Putative Stem-Like Cells. *Frontiers in Oncology* **12** (2022).

15 Hernandez-Quiles, M., Broekema, M. F. & Kalkhoven, E. PPARgamma in Metabolism, Immunity, and Cancer: Unified and Diverse Mechanisms of Action. *Frontiers in Endocrinology* **12** (2021). https://doi.org/10.3389/fendo.2021.624112

16 Mungrue, I. N., Pagnon, J., Kohannim, O., Gargalovic, P. S. & Lusis, A. J. CHAC1/MGC4505 Is a Novel Pro-apoptotic Component of the Unfolded Protein Response, Downstream of the ATF4-ATF3-CHOP Cascasde. *The Journal of Immunology* **182**, 466-476 (2009). https://doi.org/10.4049/jimmunol.182.1.466

17 Zhang, Y. *et al.* The -m6A demethylase ALKBH5□mediated upregulation of DDIT4□AS1 maintains pancreatic cancer stemness and suppresses chemosensitivity by activating the mTOR pathway. *Molecular Cancer* **21** (2022). https://doi.org/10.1186/s12943-022-01647-0

18 Goyal, B. *et al.* Diagnostic, prognostic, and therapeutic significance of long non-coding RNA MALAT1 in cancer. *Biochim Biophys Acta Rev Cancer* **1875**, 188502 (2021). https://doi.org/10.1016/j.bbcan.2021.188502

19 Gu, J. *et al.* Molecular Interactions of the Long Non-coding RNA NEAT1 in Cancer. *Cancers (Basel)* **14** (2022). https://doi.org/10.3390/cancers14164009
20 Jiang, Q., Xue, D., Shi, F. & Qiu, J. Prognostic significance of an autophagy-related long non-coding RNA signature in patients with oral and oropharyngeal squamous cell carcinoma. *Oncol Lett* **21**, 29 (2021). https://doi.org/10.3892/ol.2020.12290
21 Karpov, D. S. *et al.* LINC00973 Induces Proliferation Arrest of Drug-Treated Cancer Cells by Preventing p21 Degradation. *Int J Mol Sci* **21** (2020). https://doi.org/10.3390/ijms21218322
22 Xu, X. *et al.* A positive feedback circuit between RN7SK snRNA and m(6)A readers is essential for tumorigenesis. *Mol Ther* **31**, 1615-1635 (2023). https://doi.org/10.1016/j.ymthe.2022.12.013
23 Jiang, K. *et al.* Prognostic implications of necroptosis-related long non-coding RNA signatures in muscle-invasive bladder cancer. *Front Genet* **13**, 1036098 (2022). https://doi.org/10.3389/fgene.2022.1036098
24 Tang, M. *et al.* Potential role of lncRNA LOXL1-AS1 in human cancer development: a narrative review. *Transl Cancer Res* **13**, 1997-2011 (2024). https://doi.org/10.21037/tcr-23-1450
25 Rysz, J., Konecki, T., Franczyk, B., Lawinski, J. & Gluba-Brzozka, A. The Role of Long Non-coding RNA (lncRNAs) Biomarkers in Renal Cell Carcinoma. *Int J Mol Sci* **24** (2022). https://doi.org/10.3390/ijms24010643
26 Lu, J. *et al.* The crucial role of LncRNA MIR210HG involved in the regulation of human cancer and other disease. *Clin Transl Oncol* **25**, 137-150 (2023). https://doi.org/10.1007/s12094-022-02943-3
27 Liang, Y. *et al.* N6-methyladenosine modified lncRNAs signature for stratification of biochemical recurrence in prostate cancer. *Hum Genet* **143**, 857-874 (2024). https://doi.org/10.1007/s00439-023-02603-8
28 He, Y., Zhou, H., Xu, H., You, H. & Cheng, H. Construction of an Immune-Related lncRNA Signature That Predicts Prognosis and Immune Microenvironment in Osteosarcoma Patients. *Front Oncol* **12**, 769202 (2022). https://doi.org/10.3389/fonc.2022.769202

FIGURE LEGENDS

Figure 1. *In vitro* cell viability assays. 1A. Representative dose-response plots showing *in vitro* cytotoxicity of Clofazimine as single agent and in combination with Docetaxel (DTX) in PCa cell lines. Chemosensitivity assays were performed using Resazurin. The combination index (CI) and Dose reduction index (DRI) values were calculated using Chou-Talalay's algorithm. Figure 1B. % Apoptotic cells representing the effect of CLF on PCa cell lines as a single agent and in combination with DTX. Cells were treated for 48 hours, and then apoptosis was measured using Annexin V-FITC and flow cytometry. 1C. Representative Caspase 3/7 activity assays showing increased apoptosis following CLF treatment.

Figure 2. ALDH activity in cell lines following CLF treatment. A. DU145 B. DUTXR. C. PC3. D. PC3M. E. C4-2b. Cells were treated for 24 hr, and ALDH activity was measured using the Aldefluor assay kit and flow cytometry (DEAB: positive control).

Figure 3. Gene expression analysis: Control vs CLF treatment. 3A. Volcano plot showing the differentially expressed (DE) genes. 3B. Venn Diagram showing CLF-regulated genes that were common between the cell lines. 3C. Heatmap representing the top genes that were most significantly differentially expressed between CLF-treated vs untreated controls.

Figure 4. Ingenuity pathway analysis based on differentially expressed genes results showing, 4A. Graphical Summary; 4B. Top Canonical Pathways (B-H>1.3; |z|>2); 4C. Top predicted Upstream regulators (p-value of overlap <0.05; Predicted activation z-score & expression fold change>|1.5|).

Figure 5. CLF affects mitochondrial membrane potential (MMP) and intra-cellular reactive oxygen species (ROS) generation in PCa cells. Representative figures showing the DU145 cell lines. **A. Mitochondrial membrane potential (MMP):** JC-1 (Sigma), a cationic carbocyanine dye that accumulates in mitochondria, was used to assess Mitochondrial membrane potential ($\Delta\Psi_M$). **B. ROS generation:** DCFDA (Sigma) was used to measure intracellular ROS production by flow cytometry. DCFDA shows fluorescence when oxidized.

Figure 6. Validation of CLF treatment-related gene signatures using TCGA's prostate adenocarcinoma (PRAD) GEP dataset. Kaplan-Meier Curves show that the top CLF treatment-induced genes are significantly associated with disease-free survival in PCa patients. i) ARG2; ii) B4GALNT4; iii) BOLA2; iv) FAM111B; v) HMGN2P5; vi) LCN2; vii) RRAGD; viii) RAB39B.

Figure 7. Heatmap representing top lncRNAs and snRNAs differentially regulated following CLF treatment in mCRPC cell lines. Details are provided in Table 2.

Table 1. List of drugs and reagents used in the study.

Reagents	Manufacturer	Location
Fetal bovine serum	Hyclone (Thermo-Fisher Scientific Inc.)	Rockford, IL, USA
Trypsin (0.25% w/v)	Hyclone (Thermo-Fisher Scientific Inc.)	Rockford, IL, USA
Penicillin-Streptomycin (10,000 U/mL)	Gibco™ (Thermo-Fisher Scientific Inc.)	Waltham, MA, USA
FITC Annexin V Apoptosis Detection Kit	BD Biosciences	San Jose, CA, USA
RIPA lysis buffer	Thermo-Fisher Scientific Inc.	Waltham, MA, USA
Halt™ Protease and Phosphatase Inhibitor Cocktail	Thermo-Fisher Scientific Inc.	Waltham, MA, USA
Pierce ™ ECL Western Blotting Substrate	Thermo-Fisher Scientific Inc.	Waltham, MA, USA
RNeasy Plus Mini Kit	QIAGEN	Hilden, Germany
Quick Start Bovine Serum Albumin Standard	Bio-Rad	Hercules, CA, USA
Tris Buffer Saline (TBS)	Bio-Rad	Hercules, CA, USA
10% Tween 20	Bio-Rad	Hercules, CA, USA
Polyvinylidene fluoride membrane (PVDF)	EMD Millipore	Billerica, MA, USA
Bovine Serum Albumin (BSA)	VWR	Radnor, PA, USA
Dimethyl sulfoxide (DMSO)	Sigma-Aldrich Inc.	St. Louis, MO, USA
Bradford Reagent	Sigma-Aldrich Inc.	St. Louis, MO, USA
JC-1 - Mitochondrial Membrane Potential Assay Kit	Abcam	Waltham, MA, USA
Anti-rabbit IgG, HRP-linked Antibody (7074S)	Cell Signaling Technology	Danvers, MA, USA
β-actin (A3854) Antibody	Sigma-Aldrich Inc	St. Louis, MO, USA
Clofazimine	Selleckchem	Houston, TX, USA
Docetaxel	Selleckchem	Houston, TX, USA

Table 2: Top differentially regulated non-coding RNAs following CLF treatment ($p<0.05$).

Gene name	Chromosome	Start	Stop	Gene biotype	P-value	Log_2(Ratio)	Fold change
RN7SK	6	52995621	52995949	snRNA	2.58E-04	-8.95	-494.45
RN7SL4P	3	15738515	15738810	misc_RNA	3.61E-02	-4.32	-20.00
MALAT1	11	65497688	65506517	lncRNA	1.94E-03	-4.18	-18.06
RN7SL1	14	49586580	49586879	misc_RNA	3.54E-02	-3.09	-8.52
NEAT1	11	65422774	65445541	lncRNA	5.02E-03	-3.00	-8.01
MT-RNR1	M	648	1602	Mt_rRNA	4.99E-03	-2.76	-6.79
SAP30L-AS1	5	154325568	154445851	lncRNA	1.81E-02	-2.66	-6.33
7SK	6	52995620	52995951	misc_RNA	3.91E-03	-2.62	-6.14
MBNL1-AS1	3	152245262	152269558	lncRNA	1.09E-02	-2.51	-5.71
RNF213-AS1	17	80351828	80415169	lncRNA	1.73E-02	-2.50	-5.65
RTCA-AS1	1	100251528	100266180	lncRNA	8.14E-03	-2.10	-4.28
ZFHX2-AS1	14	23511760	23560779	lncRNA	3.98E-02	-2.09	-4.27
STAG3L5P-PVRIG2P-PILRB	7	100336104	100367832	lncRNA	2.07E-02	-2.09	-4.24
PCAT1	8	126556323	127419051	lncRNA	3.51E-02	2.02	4.04
LINC00957	7	44039171	44042307	lncRNA	6.98E-03	2.07	4.19
TMEM202-AS1	15	72407778	72475169	lncRNA	2.13E-03	2.56	5.92
MIF-AS1	22	23894426	23898931	lncRNA	4.26E-03	2.65	6.27
LINC00973	3	98981058	98983097	lncRNA	1.20E-02	2.71	6.55
MYG1-AS1	12	53298655	53300315	lncRNA	1.19E-03	2.88	7.38

Figure 1. *In vitro* cell viability assays.

1A. Representative dose-response plots showing *In vitro* cytotoxicity of Clofazimine as single agent and in combination with Docetaxel (DTX) in PCa cell lines. Chemosensitivity assays were performed using Resazurin. Combination index (CI) and Dose reduction index (DRI) were calculated using Chou-Talalay's algorithm.

A

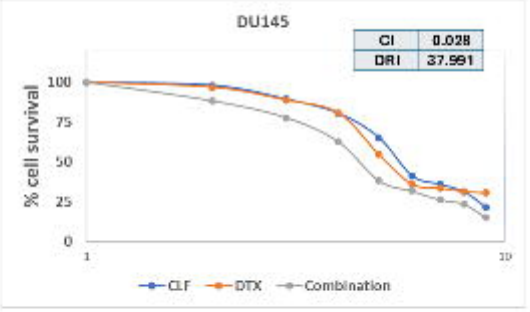

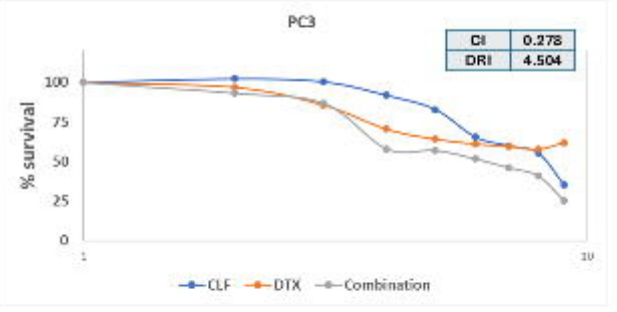

Figure 1B. % Apoptotic cells representing the effect of CLF on PCa cell lines as a single agent and in combination with DTX. Cells were treated for 48 hours, and then apoptosis was measured using Annexin V-FITC and flow cytometry.

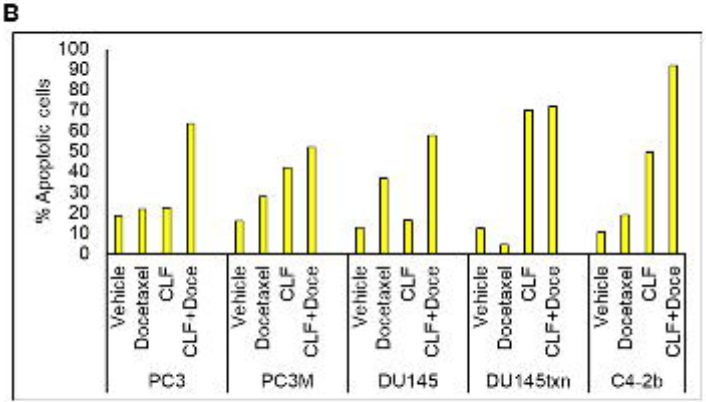

1C. Representative Caspase 3/7 activity assay plots showing increased apoptosis following CLF treatment.

C

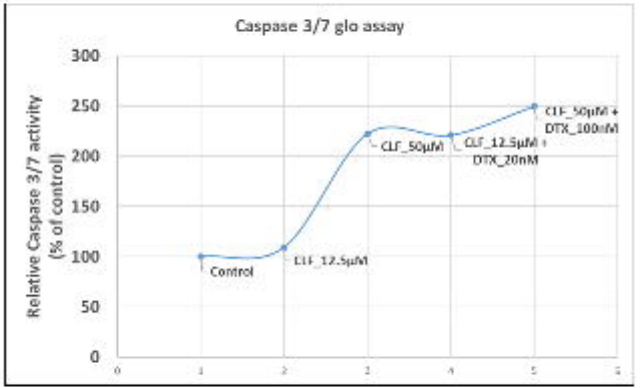

Figure 2. ALDH activity in cell lines following CLF treatment. A. DU145 B. DUTXR. C. PC3. D. PC3M. E. C4-2b. Cells were treated for 24 hr, and ALDH activity was measured using the Aldefluor assay kit and flow cytometry (DEAB: positive control).

A. DU145

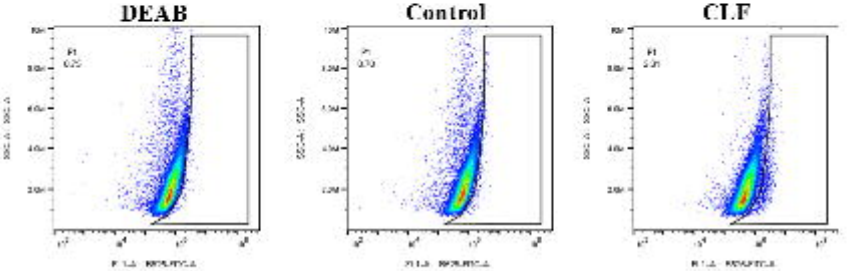

B. DU1XR

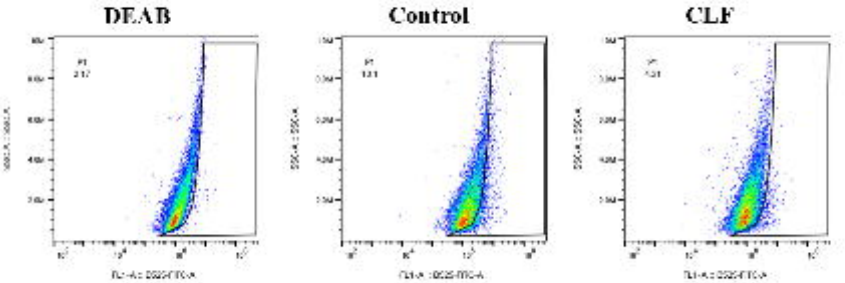

C. PC-3

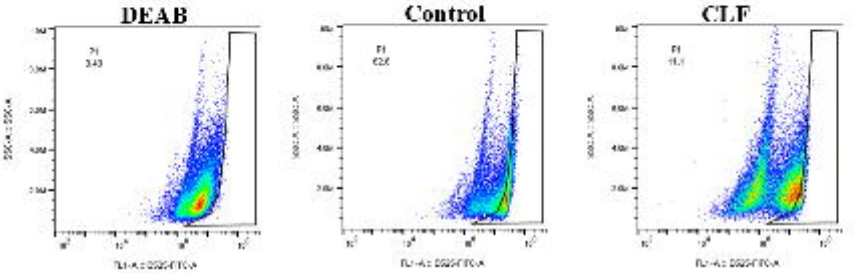

D. **PC-3M**

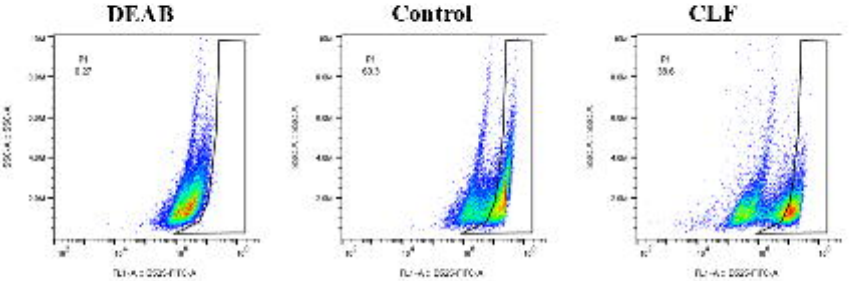

E. C4-2b

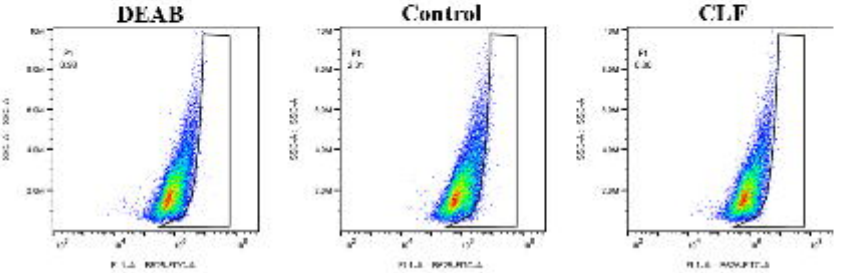

Figure 3. Gene expression analysis: Control vs CLF treatment. 3A. Volcano plot showing the differentially expressed (DE) genes.

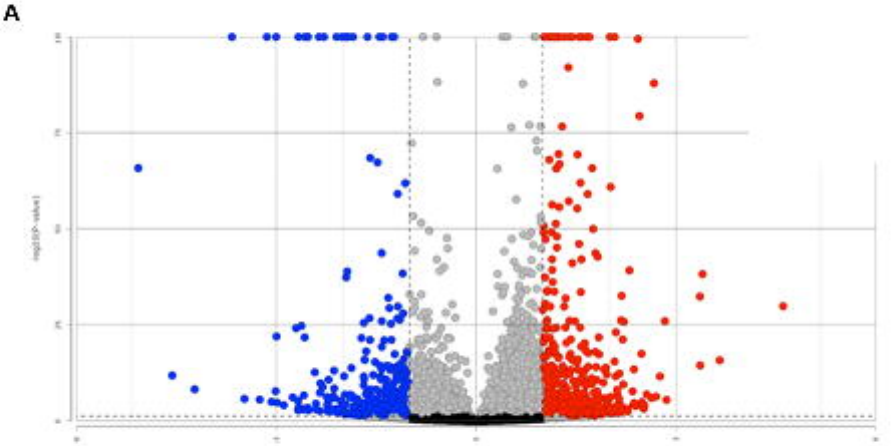

3B. Venn Diagram showing CLF-regulated genes that were common between the cell lines.

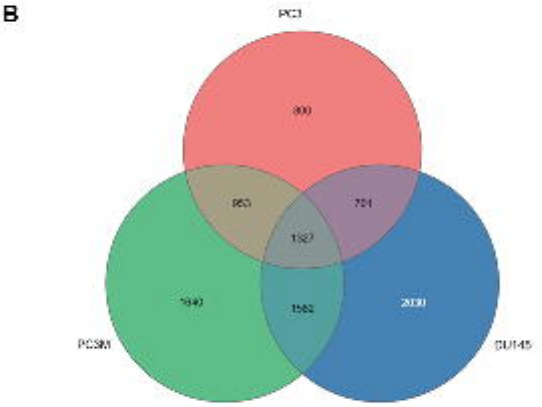

3C. Heatmap representing the top genes that were most significantly differentially expressed between CLF-treated vs untreated controls.

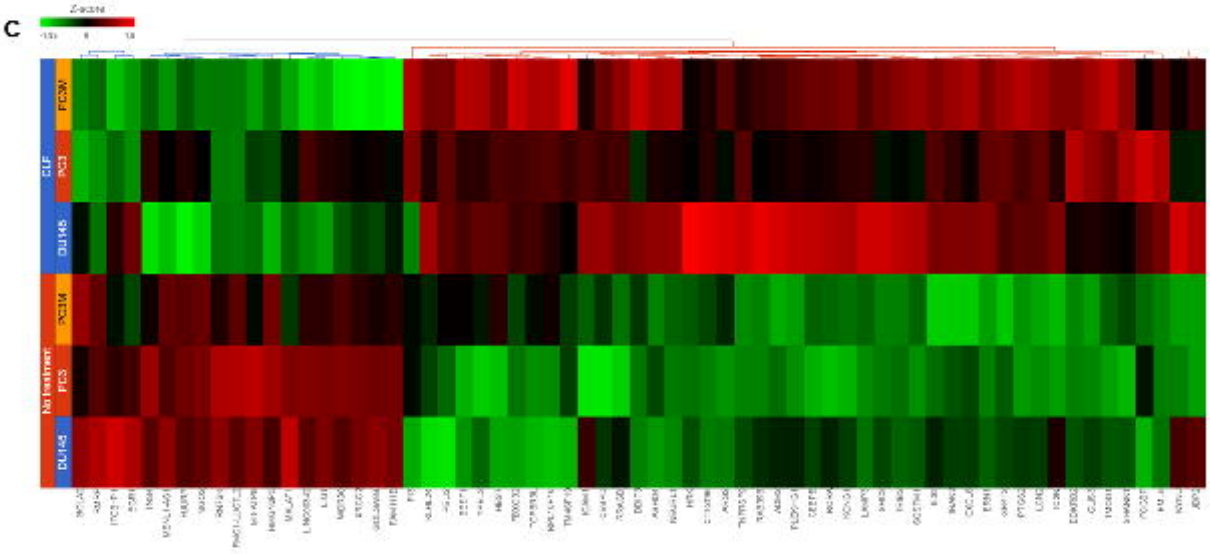

Figure 4. Ingenuity pathway analysis based on differentially expressed genes results showing,
4A. Graphical Summary

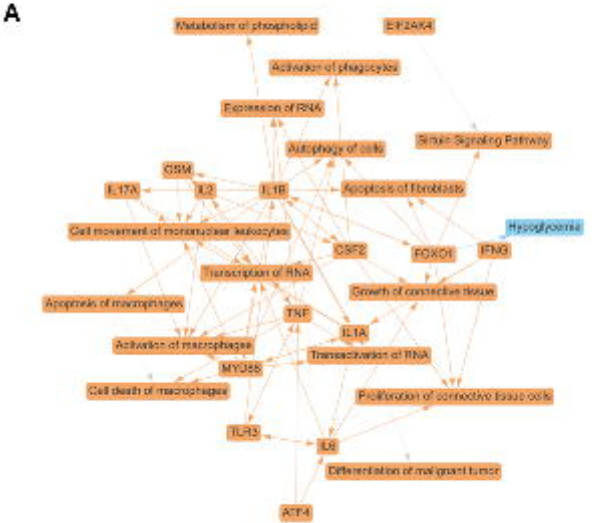

4B. Top Canonical Pathways (B-H>1.3; |z|>2);

B

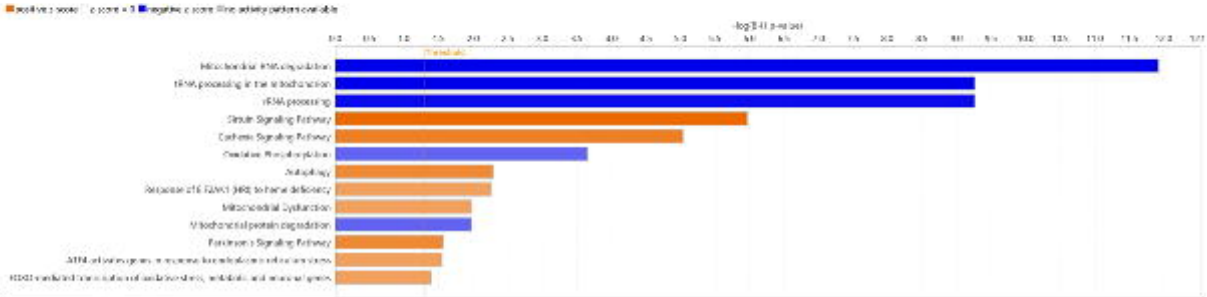

4C. Top predicted Upstream regulators (p-value of overlap <0.05; Predicted activation z-score & expression fold change>|1.5|).

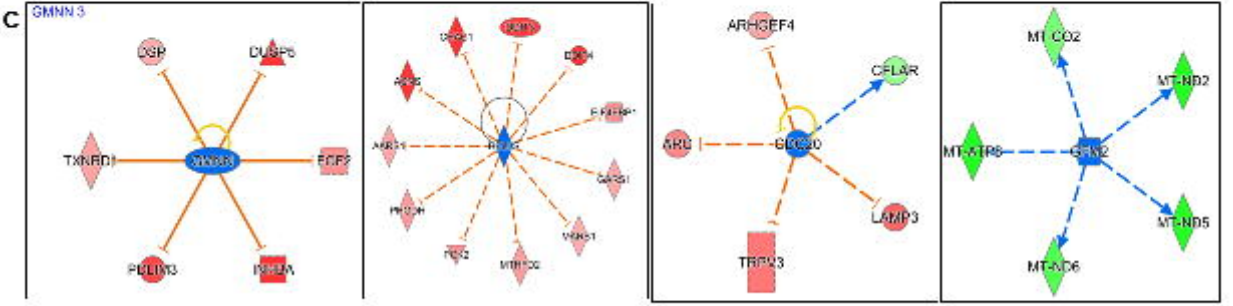

Figure 5. CLF affects mitochondrial membrane potential (MMP) and intra-cellular reactive oxygen species (ROS) generation in PCa cells. Representative figures showing the DU145 cell lines.
A. Mitochondrial membrane potential (MMP): JC-1 (Sigma), a cationic carbocyanine dye that accumulates in mitochondria, was used to assess Mitochondrial membrane potential ($\Delta\Psi_M$).

A

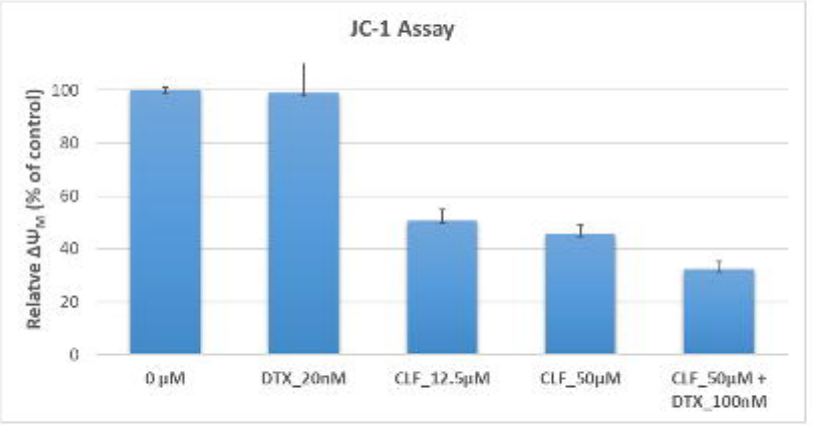

B. ROS generation: DCFDA (Sigma) was used to measure intracellular ROS production by flow cytometry. DCFDA shows fluorescence when oxidized.

B

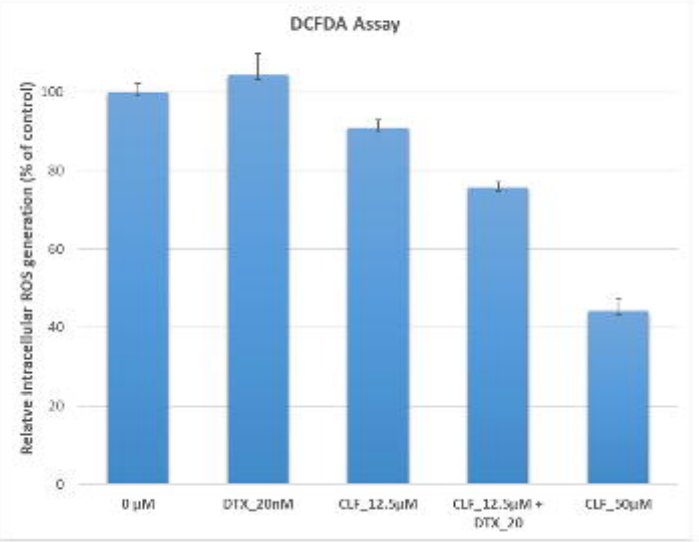

Figure 6. Validation of CLF treatment-related gene signatures using TCGA's prostate adenocarcinoma (PRAD) GEP dataset. Kaplan-Meier Curves show that the top CLF treatment-induced genes are significantly associated with disease-free survival in PCa patients. i) ARG2; ii) B4GALNT4; iii) BOLA2; iv) FAM111B; v) HMGN2P5; vi) LCN2; vii) RRAGD; viii) RAB39B.

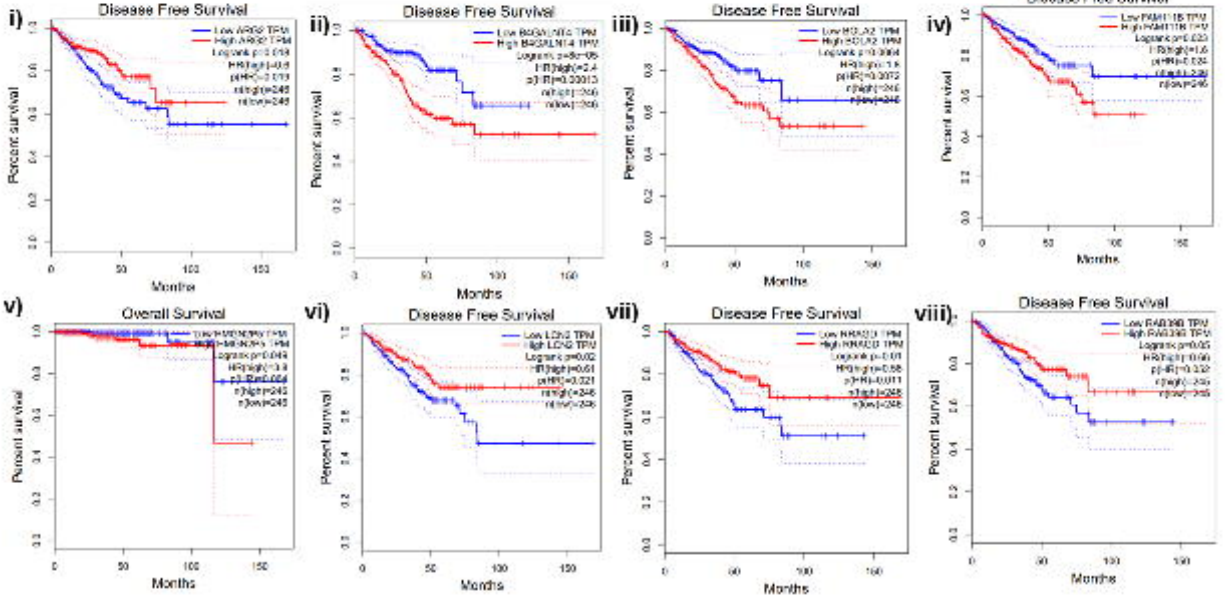

Figure 7. Heatmap representing top lncRNAs and snRNAs differentially regulated following CLF treatment in mCRPC cell lines. Details are provided in **Table 2**.